Complex Patterns of Non-Gaussian Diffusion in Artificial Anisotropic Tissue Models

Farida Grinberg[1], Ezequiel Farrher[1], Ivan I. Maximov[1], and N. Jon Shah[1,2]

[1]*Institute of Neuroscience and Medicine, Forschungszentrum Juelich, Juelich, Germany,* [2]*Faculty of Medicine, JARA, RWTH Aachen University, Aachen, Germany*

Target Audience

The target audience of this abstract are researchers investigating water diffusion properties in biological tissues.

Purpose

Complex cellular microstructure in the biological tissue gives rise to non-Gaussian patterns of water diffusion. Cell or fibre packing density is one of the important factors that determines the tortuosity of the porous space and affects diffusion properties (consider, for example, axonal losses associated with neurodegenerative diseases and traumatic brain injuries or cell swelling in stroke). In order to better understand the fundamental effects of microstructure on the response signal we have studied less complex model systems with well-defined properties, such as a recently developed synthetic anisotropic fibre phantom, Figure 1, which mimics the extracellular space in the brain white matter. The phantom exhibits a region with the gradient of the fibre packing density, *f*. The primary purpose of this study was to perform a comparative analysis of the influence of fibre density on the quantitative metrics in the three non-Gaussian models recently introduced in the brain research: the diffusion kurtosis model (Jensen, et al., MRM, 2005), DKM, the lognormal-distribution model[2], LNDM, and the stretched-exponential model[3], SEM. We also analyse the time-dependent behaviour of axial, λ_{axial}, (parallel to fibres), and radial, λ_{radial}, (perpendicular to fibres) diffusivities in the frame of the anomalous diffusion model.

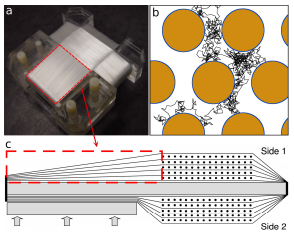

Figure 1. Fibre phantom (a) with the gradient of fibre density (c); diffusion takes place in the interstitial space (b).

Materials and Methods

The construction of a fibre phantom with a fibre-density gradient, as well as the diffusion experiments performed on it, are described in Ref.[1]. The stimulated echo pulse sequence was used for time-dependent studies of λ_{axial} (the major tensor eigenvalue) and λ_{radial} (the average of two minor eigenvalues) derived by a tensor reconstruction for typical $b \leq 1$ μm^{-2} ms. Diffusion attenuation curves in the direction perpendicular to the fibre axis (maximum hindrance) were measured using a double-refocused spin-echo pulse sequence and analyzed in the range of $b \leq 7$ μm^{-2} ms with LNDM (Eqs. (3-5) in Ref.[2]) and SEM (Eq. (3) in Ref.[3]), and in the reduced range of $b \leq$ 2.5 μm^{-2} ms with DKM (Eq. (1) in Ref.[1]). The fitting parameters are denoted as follows: D_k (the mean diffusivity, DKM), D_{ld} (the peak diffusivity, LNDM), and D_{se} (the distributed diffusion coefficient, SEM), K (the mean excess kurtosis, DKM), σ (the width of the distribution function, LNDM), and α (the stretching exponent, SEM). K, σ, and α characterize the deviations from the Gaussian model (K=0, σ=0, and α=1).

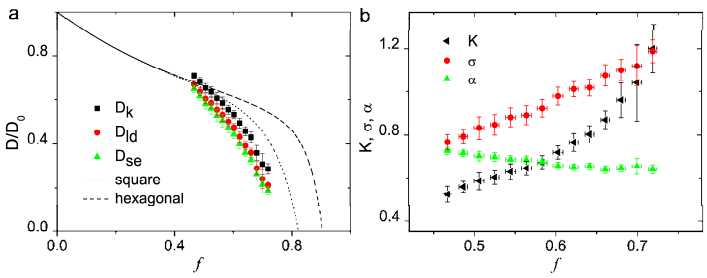

Figure 2. Normalised diffusivities (a) and K, α, σ (b) as a function of f. The curves in (a) are theoretical predictions based on the Maxwell-Garnett equation (fourth order) for a hexagonal (dashed) and square (dotted) packs.

Results and Discussions

Figures 2a and 2b show the fitted parameters as a function of f in the range from 0.46 to 0.71. In this range, the values of D_k, D_{ld}, and D_{se} decreased by factors 2.4, 3.1, and 3.4, respectively, the values of K and σ increased by a factor of $\approx$2.3 and $\approx$1.5, respectively, and α decreased by a factor of $\approx$ 1.13. An interesting finding is that the largest change in the "non-Gaussianness" parameter (K) is accompanied with the smallest change in the diffusivity (D_k), whereas the largest change in the diffusivity (D_{se}) is related to the smallest change in α. Thus, all models are complementary with respect to sensitivity to f and related imaging contrasts. In comparison to the theoretical curves (Sen and Basser, MRI, 2005), a steep decrease of the diffusivities occurs at smaller f (~ 0.7) than predicted for a hexagonal or square packing geometries on approaching the critical close pack values of 0.785 (square) or 0.90 (hexagonal). This lower value is in a good agreement with the close pack density for random cylinder packing relevant for our phantom. Figure 3a shows λ_{axial} and λ_{radial} as a function of the diffusion time, t_d, in the double logarithmic scale. λ_{axial} was close to the bulk water diffusivity independent of f indicating, as expected, unrestricted diffusion along the fibres. In contrast, λ_{radial} as a function of t_d is described by the power-law function, $\lambda_{radial} \propto t_d^{\gamma}$, (solid lines) in the range of times exceeding one order of the magnitude (0.042 s – 1.024 s). This range can be considered "intermediate" between the short- and long-time limits. The slopes were larger the higher fibre density. Figure 3b shows the fitted values of γ as a function of f. For f ~< 0.58, γ exhibits a slight linear decrease with f but a steep decrease for higher values. Interestingly, this quasi-critical behaviour of γ is different from that of the above non-Gaussian metrics that exhibit more gradual change with f. These and related results are discussed in terms of the underlying mechanisms, i.e. anomalous diffusion in restricted geometries, and their relevance for better understanding potential diffusion contrasts in the fibrous tissue.

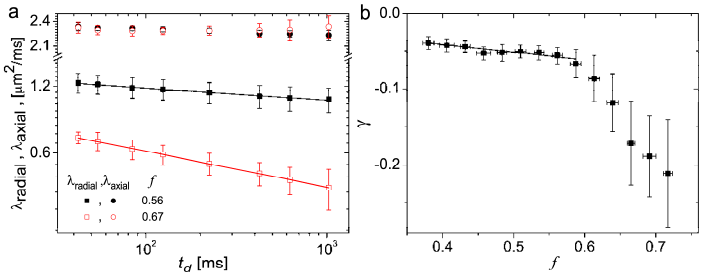

Figure 3. λ_{axial} and λ_{radial} as a function of t_d (a) and the dependence of γ on f (b).

Conclusions

We demonstrated that all models provide parameters sensitive to fibre density and, thus, potential biomarkers of axonal losses/damage in pathological tissue conditions. Neither of the three non-Gaussian models has demonstrated a superior sensitivity of both free parameters simultaneously, therefore, all models are complementary to each other. Due to its critical-like behaviour, the power-law exponent in the anomalous diffusion model occurs mostly sensitive to f in a certain range of values well below the close pack.

References

[1] E. Farrher, J. Kaffanke, A.A. Celik, T. Stocker, F. Grinberg, N.J. Shah, Novel multisection design of anisotropic diffusion phantoms, Magn. Reson. Imaging, 30 (2012) 518-526; [2] F. Grinberg, L. Ciobanu, E. Farrher, N.J. Shah, Diffusion kurtosis imaging and log-normal distribution function imaging enhance the visualisation of lesions in animal stroke models, NMR Biomed, 25(2012) 1295-304; [3] K.M. Bennett, K.M. Schmainda, R.T. Bennett, D.B. Rowe, H. Lu, J.S. Hyde, Characterization of continuously distributed cortical water diffusion rates with a stretched-exponential model, Magn. Reson. Med., 50 (2003) 727-734.